Ocean heat storage rate unaffected by MOC weakening in an idealized climate model

Geophysical Research Letters

RESEARCH LETTER
10.1029/2020GL089849

Ocean Heat Storage Rate Unaffected by MOC Weakening in an Idealized Climate Model

Peter Shatwell[1], **Arnaud Czaja**[1], **and David Ferreira**[2]

[1]Department of Physics, Imperial College London, London, UK, [2]Department of Meteorology, University of Reading, Reading, UK

Key Points:
- A deep meridional overturning circulation (MOC) connects the ocean surface to its interior, enhancing heat storage rate under global warming
- This circulation in the Atlantic (AMOC) may enable its enhanced heat storage rate relative to the Pacific in recent decades
- MOC weakening does not necessarily impact ocean heat storage rate due to compensating physical processes

Supporting Information:
- Supporting Information S1

Correspondence to:
P. Shatwell,
peter.shatwell12@imperial.ac.uk

Citation:
Shatwell, P., Czaja, A., & Ferreira, D. (2020). Ocean heat storage rate unaffected by MOC weakening in an idealized climate model. *Geophysical Research Letters*, *47*, e2020GL089849. https://doi.org/10.1029/2020GL089849

Received 15 JUL 2020
Accepted 27 JUL 2020
Accepted article online 4 AUG 2020

Abstract To study the role of the Atlantic meridional overturning circulation (AMOC) in transient climate change, we perform an abrupt CO_2-doubling experiment using a coupled atmosphere-ocean-ice model with a simple geometry that separates the ocean into small and large basins. The small basin exhibits an overturning circulation akin to the AMOC. Over the simulated 200 years of change, it stores heat at a faster rate than the large basin by $0.6 \pm 0.2\,\mathrm{W\,m^{-2}}$. We argue that this is due to the small basin MOC. However, we find that as the MOC weakens significantly, it has little impact on the small basin's heat storage rate. We suggest this is due to the effects of both compensating warming patterns and interbasin heat transports. Thus, although the presence of a MOC is important for enhanced heat storage, MOC weakening is surprisingly unimportant.

Plain Language Summary The oceans take up the vast majority of the excess heat energy due to global warming. An important large-scale ocean circulation is the Atlantic meridional overturning circulation (AMOC). Under global warming, it has been suggested that this circulation is important for storing excess heat energy in the deep ocean. Some evidence suggests that the AMOC has weakened since the mid-twentieth century, and surface warming may intensify in response to the Atlantic storing less excess heat energy in the deep ocean. In order to examine this process more closely, we use a simple computer model of a world with no land masses and only two ocean basins: a small basin with a circulation similar to the AMOC, and a large basin without, similar to the Pacific. We approximate global warming by increasing the CO_2 in the model atmosphere and find that the small basin stores heat at a faster rate than the large basin. The small basin's overturning circulation does weaken, but this weakening does not affect the small basin's heat storage rate. This is a surprising result and casts doubt on the idea that AMOC changes will significantly enhance surface warming as the Earth warms.

1. Introduction

Due to anthropogenic carbon emissions, there is now greater absorbed solar radiation than outgoing longwave radiation over the surface of the Earth, leading to an imbalance, designated Earth's energy imbalance (EEI) (Hansen et al., 2011; Trenberth et al., 2014; Von Schuckmann et al., 2016). The vast majority (~93%) of the excess energy resulting from this imbalance manifests as an increase in ocean heat content (OHC) (Rhein, 2013). Improving estimates of OHC has been highlighted as critical to constraining EEI and thus understanding Earth's heat storage (Von Schuckmann et al., 2016).

Ocean heat uptake (OHU) acts as a buffer for surface warming. If more energy is taken into the ocean interior below the mixed layer, then less is absorbed at the atmospheric surface; indeed, so-called "surface warming hiatuses" have been linked to periods of enhanced ocean heat uptake (Drijfhout et al., 2014; Meehl et al., 2011; Watanabe et al., 2013). Recently, more attention has been drawn to the role of ocean circulation on heat uptake (e.g., Marshall et al., 2015; Winton et al., 2013), particularly that of the Atlantic's meridional overturning circulation (AMOC). It is possible that the presence of this circulation gives the Atlantic its enhanced heat storage rate compared to the Pacific, as seen in observations (e.g., Chen & Tung, 2014; Desbruyeres et al., 2017; Zanna et al., 2019).

The depth and strength of the AMOC positively correlates with the depth of global ocean heat storage (OHS) across models participating in the fifth phase of the Coupled Model Intercomparison Project (CMIP5) (Kostov et al., 2014). Multidecadal variability of the AMOC has been linked to periods of enhanced global surface warming and cooling (Chen & Tung, 2018). The AMOC's role in global OHS is especially

interesting due to the possibility of it weakening in the future. A weakening response of the AMOC with global surface warming is seen across CMIP5 models (Weaver et al., 2012), and indirect proxy observations point to the AMOC having weakened since the mid-twentieth century (Caesar et al., 2018). Model biases may favor a stable AMOC, and it is still a concern that the AMOC could collapse in the future, leading to abrupt changes in climate (Caesar et al., 2018; Liu et al., 2017).

A weakening AMOC results in a weakening of the northward oceanic meridional heat transport (MHT), which may explain the conspicuous region of cooling in the subpolar North Atlantic found in maps of temperature trends (Rahmstorf et al., 2015). It has been suggested that this North Atlantic surface cooling reduces the annual-mean sea-air temperature difference and so reduces the sensible heat flux from the ocean to the atmosphere, leading to an increase in ocean heat uptake (Drijfhout et al., 2014; Winton et al., 2013). Thus, OHU and OHS are quite different, as here, a local *increase* in OHU associated with a weakening AMOC could possibly be accompanied by a global *decrease* in OHS, due to ocean heat transport divergences.

Recent work (Saenko et al., 2018) has cast doubt on the observed model correlation between AMOC strength and heat storage (Kostov et al., 2014), suggesting that the eddy parameterization affects both AMOC strength and global OHU efficiency, thus causing a spurious correlation between the two quantities. But without a better conceptual grasp on how the AMOC affects OHS, it is unclear whether this correlation is spurious or not. Furthermore, these studies (Kostov et al., 2014; Saenko et al., 2018) establish a link between the AMOC and *global* OHS, while it may be easier to first consider the AMOC's influence on heat storage within the Atlantic basin itself. Given the importance of constraining and monitoring EEI through OHC observations, and the possibility that the AMOC may continue to weaken into the future, it is imperative to better understand the AMOC's role in ocean heat uptake and storage as the world continues to warm.

To this end, we examine the response of a coupled atmosphere-ocean-ice general circulation model under an abrupt doubling of atmospheric CO_2. The model geometry invokes two sea floor to sea surface meridional barriers that separate the ocean into small (SB) and large basins (LB). The SB exhibits an overturning circulation akin to the AMOC, while the LB does not. We look at the basins' individual responses rather than taking a global perspective, and we isolate the effect of the SB MOC by focusing on SB-LB differences. We describe the model formulation and geometry in section 2. In section 3, we present results from the abrupt CO_2-doubling experiment where we find and define a heat storage contrast between the SB and LB. We explore the role of the SB's MOC in establishing this contrast, particularly its time evolution as the MOC weakens. We also present preliminary results from four CMIP5 models demonstrating the existence of a heat storage contrast between the Atlantic and Pacific basins in abrupt CO_2-quadrupling experiments, which parallels the contrast between our model's SB and LB. Conclusions are presented in section 4.

2. Model Description and Setup

The model uses the Massachusetts Institute of Technology general circulation model (MITgcm) code (Marshall, Adcroft, et al., 1997; Marshall, Hill, et al., 1997). Both the atmosphere and ocean component models use the same cubed-sphere grid (Adcroft et al., 2004) at a C24 resolution (24×24 points per face, giving a resolution of 3.75° at the equator). The atmosphere has a low vertical resolution of five levels, and its physics is based on the "simplified parameterizations primitive-equation dynamics" (SPEEDY) scheme (Molteni, 2003). The ocean is flat-bottomed with a constant depth of 3 km and is split into 15 levels with increasing vertical resolution from 30 m at the surface to 400 m at depth.

Mesoscale eddies are parameterized as an advective process (Gent & Mcwilliams, 1990) and an isopycnal diffusion (Redi, 1982), both with a transfer coefficient of $1{,}200\ m^2\ s^{-1}$. Ocean convection is represented by an enhanced vertical mixing of temperature and salinity (Klinger et al., 1996), while the background vertical diffusion is uniform and set to $3 \times 10^{-5}\ m^2\ s^{-1}$. There are no sea ice dynamics, but a simple two and a half layer thermodynamic sea ice model (Winton, 2000) is incorporated. The seasonal cycle is represented, but there is no diurnal cycle.

The model is configured with the idealized "Double-Drake" (DDrake) geometry as seen in previous work (e.g., Ferreira & Marshall, 2015; Ferreira et al., 2010, 2015), which is an aquaplanet with two narrow vertical barriers that extend from the sea floor to the sea surface. The barriers are set 90° apart at the North Pole and extend meridionally to 35°S. This separates the ocean into one SB and one LB, with both of

them connected by a "southern ocean" region south of 35°S. The SB and LB in this configuration exhibit distinctive Atlantic-like and Pacific-like characteristics, with the SB being warmer and saltier, and exhibiting a deep interhemispheric MOC. This MOC is defined using a residual mean overturning between resolved and eddy-induced circulations (see Text S1 and Figure S1 in the supporting information). The model geometry captures two important asymmetries relevant to the Earth's climate: a zonal asymmetry splitting the ocean into small and large basins, and a meridional asymmetry allowing for circumpolar flow in the Southern Hemisphere, but not in the Northern Hemisphere.

The model is spun up for 6,000 years until a statistically steady state is reached. The time-mean of the last 50-year integration is used as the equilibrated control climate state. We abruptly change the longwave absorption in the CO_2 band, causing an initial top-of-atmosphere forcing (EEI) of approximately 4.4 W m^{-2}, thus mimicking an abrupt doubling of atmospheric CO_2 (Myhre et al., 1998), and run for an additional 200 years. The imposed EEI results in a warming of the climate system, and we diagnose the ensuing responses of the SB and LB relative to the control climate. In response to the CO_2 doubling, an arbitrary quantity $C = C(t, x, y, z)$ in the model changes from its control value $\overline{C}(x, y, z)$ to a perturbed value $C^{pert}(t, x, y, z)$ by an amount $\Delta C(t, x, y, z) = C^{pert} - \overline{C}$, where $\overline{C}$ is a 50-year time average.

3. Results

3.1. SB and LB Heat Storage Rates

The SB stores heat at a faster rate than the LB, and both heat storage rates decrease with time, reflecting the adjustment to a new equilibrium (Figure 1a). The LB's surface area is 3 times larger than that of the SB, yet it only takes up 2.21 times more heat energy in joules over the course of the simulation. By considering areal proportions of the total global OHC increase, we find that this is due to a combination of the SB taking up more heat than expected for its size, and the LB taking up less than expected (see Figure S2 in the supporting information).

To compare the two basins' efficiencies in storing heat, we look at basin OHC changes divided by the respective basin's surface area (in J m^{-2}). After 200 years' warming, the final anomalous OHC difference, $\Delta\mathrm{OHC}_{SB} - \Delta\mathrm{OHC}_{LB}$, is 3.45×10^9 J m^{-2} (Figure 1b), and in terms of heat storage *rates* in W m^{-2}, this translates to a time-mean heat storage contrast of 0.6 ± 0.2 W m^{-2} (Figure 1c, the difference between the red and blue curves in Figure 1a). There is large interannual variability in the heat storage rates, and the heat storage contrast shows no discernible trend over the 200 years. At the same time, we see that the SB MOC strength (stream function maximum, see Text S1 in the supporting information) weakens rapidly by ~25% during the first 30 years (Figure 1d), after which it remains quite stable at ~19 Sv (1 Sv $\equiv 10^6$ m^3 s^{-1}), with small oscillations of ~1 Sv, which likely reflect internal oscillations of the system (see Buckley et al., 2012).

3.2. Role of the SB MOC

To make the connection between ocean heat storage and the SB MOC, we look at the spatial pattern of the vertically averaged potential temperature response $\Delta\theta$ for different depth intervals (Figures 2a and 2b). The upper 1 km reveals pronounced warming at high latitudes in every basin, a conspicuous pool of warming at 40–60°N in the SB, and enhanced warming at 40°S where there is zonal circumpolar flow, a feature reminiscent of the warming behavior along the Antarctic Circumpolar Current (ACC) (Armour et al., 2016). Below 1 km depth, the temperature anomaly in the SB flows along the deep western boundary current, coincident with the lower limb of its MOC. Note there are no large temperature anomalies at depth in the LB or southern ocean regions.

The MOC's role is made even clearer when we plot the control residual overturning ($\overline{\Psi_{res}}$) on top of the final zonally averaged $\Delta\theta$ in the SB (Figure 2c). There is distinctive deep warming at 60–80°N, collocated with the downwelling branch of $\overline{\Psi_{res}}$. The $\Delta\theta$ structure also approximates the pattern of the streamlines, and we see an isolated pool of warm water between 1 and 1.5 km depth near the equator, suggesting the equatorward advection of temperature anomalies into this region away from the high latitudes of deep water formation.

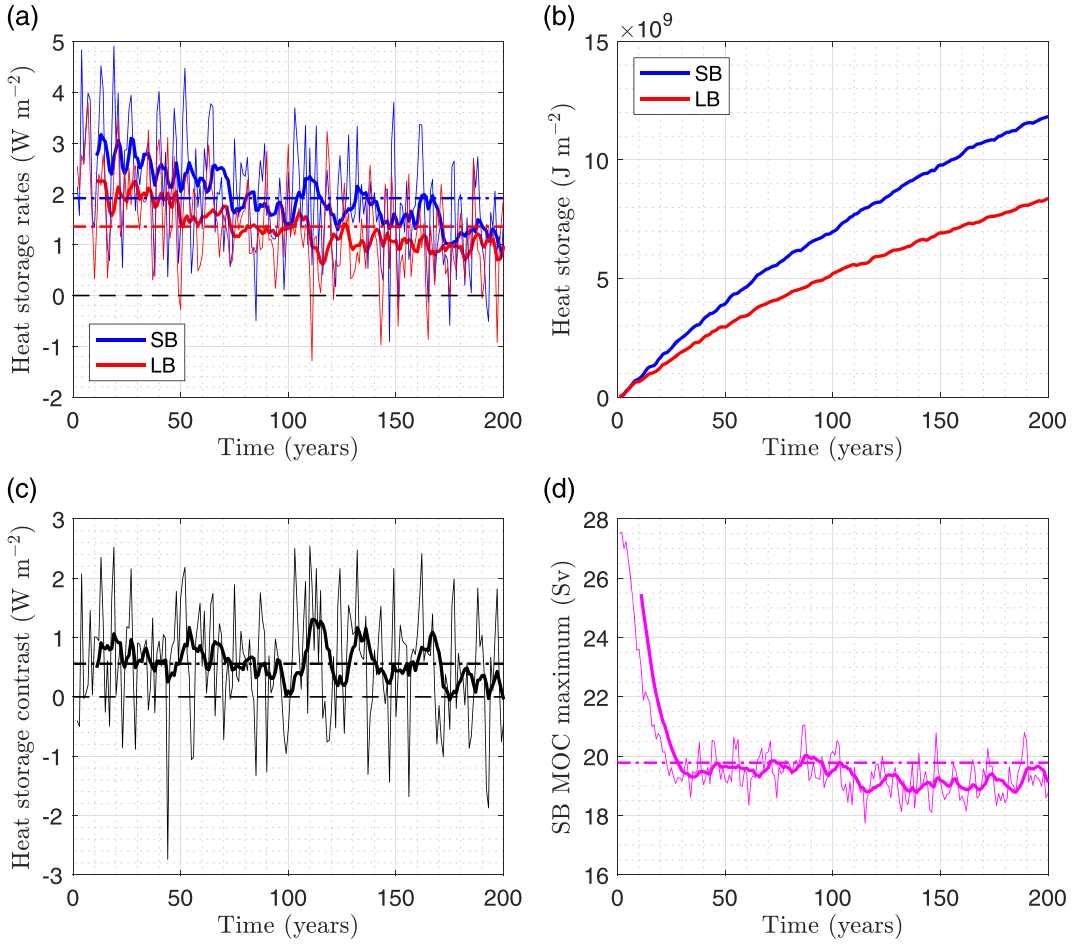

Figure 1. Time series of annually averaged (a) SB and LB heat storage rates ($\partial_t(\Delta\text{OHC})$, in W m^{-2}); (b) OHC anomalies (ΔOHC, in J m^{-2}); (c) the difference in heat storage rates, that is, the heat storage contrast ($\partial_t(\Delta\text{OHC}_{SB}$ - $\Delta\text{OHC}_{LB})$, in W m^{-2}); and (d) SB MOC strength (max(Ψ_{res}^{pert}), in Sv) following an abrupt doubling of CO_2. Thick lines are decadal running means and horizontal dash-dotted lines indicate time-mean values. The time-mean heat storage contrast is 0.6 ± 0.2 W m^{-2} (standard error, assuming 20 degrees of freedom accounting for decadal oscillations).

Figures 1 and 2 together highlight that the key process governing the enhanced heat storage rate in the SB is the rapid advection of surface temperature anomalies into the interior by the MOC. This relationship between the SB's MOC and heat storage rate highlights the importance of the present-climate AMOC, which could help explain the Atlantic's observed enhanced warming rate compared to the Pacific (Chen & Tung, 2014; Desbruyeres et al., 2017; Zanna et al., 2019).

3.3. Heat Storage Response to MOC Weakening

From the previous section, it is clear that the SB MOC plays an important role in setting the heat storage contrast between the two basins of DDrake. However, the SB MOC strength weakens rapidly by ~25% during the first 30 years, after which it remains stable between 18 and 20 Sv (Figure 1d). The heat storage contrast, however, remains approximately constant over the 200 years (Figure 1c). Thus, we find that the MOC weakening has little, if any, impact on the heat storage contrast.

To explain this counterintuitive result, consider the vertical heat flux associated with the SB MOC, approximated by $\rho_0 c_p \Psi_{res} \delta\theta$ (in W), where $\rho_0 = 1{,}030$ kg m^{-3} is a reference seawater density, $c_p = 3994$ J K^{-1} kg^{-1} is the specific heat capacity of seawater (at constant pressure), and $\delta\theta$ is the temperature difference (in K) across the downwelling and upwelling branches of the circulation, that is, $\theta_\downarrow - \theta_\uparrow$. This choice is motivated by similar scaling arguments used to represent the MHT associated with the AMOC (e.g., Buckley &

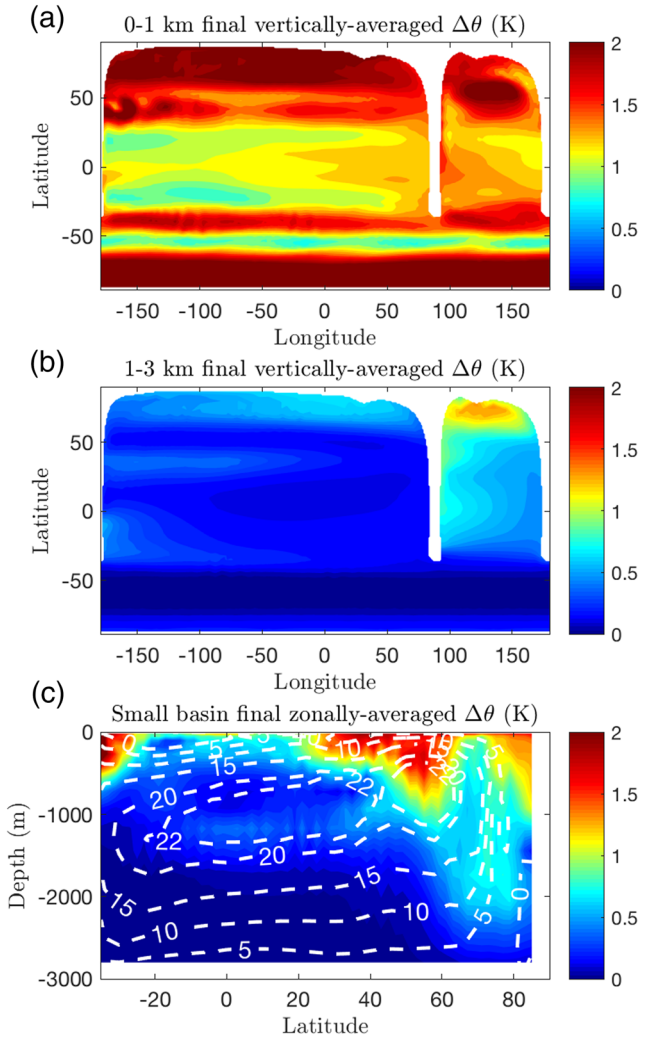

Figure 2. Vertically averaged $\Delta\theta$ (in K) after 200 years following an abrupt doubling of atmospheric CO_2 in DDrake for the depth intervals (a) 0–1 and (b) 1–3 km. The temperature anomaly at depth follows a deep western boundary current in the small basin. (c) Zonally averaged $\Delta\theta$ (color, in K) in the small basin after 200 years' warming, and streamlines (white dashed contours, in Sv) for the control residual overturning $\overline{\Psi_{res}}$.

Marshall, 2016). We take vertically averaged θ values in the latitude bands 60–80°N and 30–50°S in the SB sector for $\theta_{\downarrow}$ and $\theta_{\uparrow}$, respectively. Following the CO_2- doubling, we consider the change in the MOC heat flux, $\Delta\mathscr{H}_{MOC} = \rho_0 c_p \Delta(\Psi_{res}\delta\theta)$. This is given by (see Text S3 in the supporting information):

$$\frac{\Delta\mathscr{H}_{MOC}}{\rho_0 c_p} \approx \underbrace{\overline{\Psi_{res}}\Delta(\delta\theta)}_{>0} + \underbrace{\Delta\Psi_{res}\overline{\delta\theta}}_{>0} + \underbrace{\Delta\Psi_{res}\Delta(\delta\theta)}_{<0} \tag{1}$$

where we take the convention that a downward heat flux is positive. There are two processes to consider: one due to $\Delta\Psi_{res}$ (MOC weakening) and one due to $\Delta(\delta\theta)$ (differential warming). We find that $\theta_{\downarrow}$ warms at a faster rate than $\theta_{\uparrow}$, so that $\Delta(\delta\theta) > 0$ (see Figure S3 in the supporting information). The first term in Equation 1 is then positive, leading to an increase in the anomalous downward heat flux.

Now, we know that the MOC weakens ($\Delta\Psi_{res} < 0$), so one might think that this process compensates the differential warming (as $\Delta(\delta\theta) > 0$). Importantly, however, in the control integration, $\overline{\delta\theta} = -0.70$ K (< 0), indicating that the MOC is thermally direct and transports heat *upwards*. So, the second term in Equation 1 is in

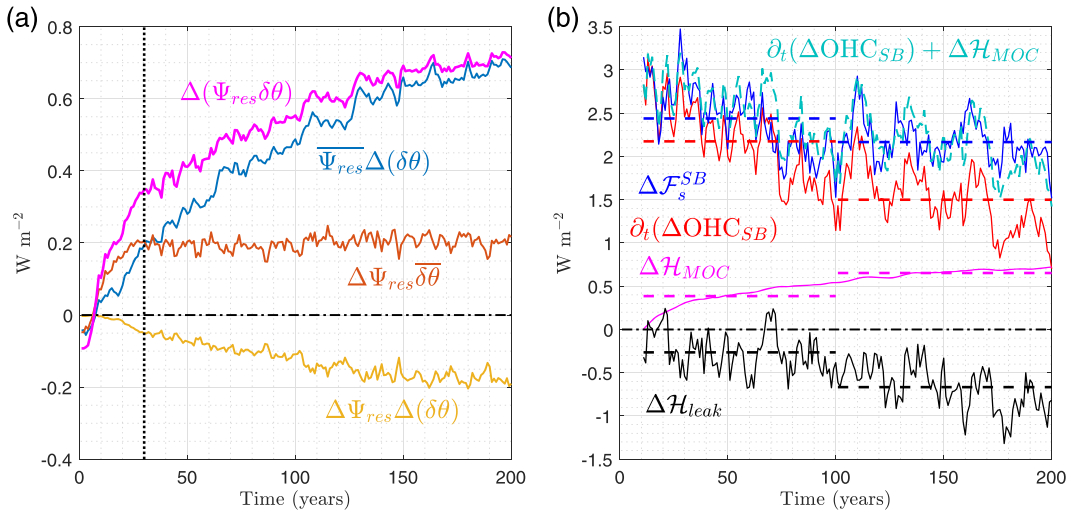

Figure 3. (a) Decomposition of the change in SB downward (positive) MOC heat flux ($\Delta(\Psi_{res}\delta\theta)$, magenta) into differential warming ($\overline{\Psi_{res}}\Delta(\delta\theta)$, blue), MOC weakening ($\Delta\Psi_{res}\overline{\delta\theta}$, orange), and nonlinear ($\Delta\Psi_{res}\Delta(\delta\theta)$, yellow) terms (annual averages, in W m^{-2}). A vertical dotted line is plotted at 30 years to separate the weakening and non-weakening MOC regimes. (b) Decadal running means of the SB heat uptake rate ($\Delta\mathcal{F}_s^{SB}$, blue), heat storage rate ($\partial_t(\Delta OHC_{SB})$, red), MOC heat flux ($\Delta\mathcal{H}_{MOC}$, magenta), and leakage rate to the southern ocean region ($\Delta\mathcal{H}_{leak} = \partial_t(\Delta OHC_{SB}) - \Delta\mathcal{F}_s^{SB}$, black) (in W m^{-2}). Note that the sum of the heat storage rate and MOC heat flux (light blue, dashed) almost matches the heat uptake rate. Horizontal dashed lines are centennial time means.

fact *positive*. We can conclude this more directly if we project the circulation into depth-temperature coordinates, using methods from Zika et al. (2013), demonstrating that the downwelling occurs at a cooler temperature than the upwelling (see supporting information).

Both the differential warming *and* the MOC weakening processes thus contribute to an *increase* in the anomalous downward heat flux. Only their interaction $\Delta\Psi_{res}\Delta(\delta\theta)$ is negative, leading to an upward heat flux. Overall, this means that $\Delta\mathcal{H}_{MOC} > 0$. These terms are plotted (in W m^{-2}) in Figure 3a. Notably, the two terms involving $\Delta\Psi_{res}$ (i.e., MOC weakening) compensate each other, while the dominant term is $\overline{\Psi_{res}}\Delta(\delta\theta)$, so it is the control overturning that plays the prominent role. We acknowledge that equation 1 assumes that the latitudinal structures of $\Delta\Psi_{res}$ and $\overline{\Psi_{res}}$ are similar, and this assumption is not entirely appropriate during the period of MOC weakening (see Figure S4 in the supporting information). However, it is appropriate during the non-weakening regime, and so our results—the $\Delta\Psi_{res}\overline{\delta\theta}$ and $\Delta\Psi_{res}\Delta(\delta\theta)$ terms compensate each other, and $\Delta\mathcal{H}_{MOC}$ increases with time—are robust.

The anomalous downward MOC heat flux increases with time, and most rapidly during the MOC weakening. Why this increase in $\Delta\mathcal{H}_{MOC}$ does not lead to an increase in the heat storage contrast remains to be explained. If we consider the increase in air-sea heat flux (heat uptake) compared to the increase in OHC (heat storage) in the SB, we find that the SB *leaks heat* across 35°S to the southern ocean region at a rate of ~0.5 W m^{-2}, and this leakage rate increases with time (Figure 3b). For a change in OHC in the SB, we can write

$$\partial_t(\Delta\mathrm{OHC}_{SB}) = \Delta\mathcal{F}_s^{SB} \underbrace{+\rho_0 c_p \int_{\text{at } 35°\text{S}} \int_{-H_{SB}}^{0} \Delta(v\theta_{SB})\, dz\, dx}_{\Delta\mathcal{H}_{leak}} \tag{2}$$

where $\Delta\mathcal{F}_s^{SB}$ is the change in net surface heat flux over the SB, H_{SB} is the SB depth, and we define $\Delta\mathcal{H}_{leak}$ as the SB heat leakage rate across 35°S. From Figure 3b, we see that $\Delta\mathcal{H}_{leak}$ and $\Delta\mathcal{H}_{MOC}$ compensate each other, especially on long timescales (see dashed lines). This is made even clearer in an energy budget sense, where we find that $\partial_t(\Delta OHC_{SB}) + \Delta\mathcal{H}_{MOC} \approx \Delta\mathcal{F}_s^{SB}$ (light blue, dashed), which implies that $\Delta\mathcal{H}_{MOC} \approx -\Delta\mathcal{H}_{leak}$. So, as the SB MOC heat flux increases, this permits more heat to penetrate the ocean surface,

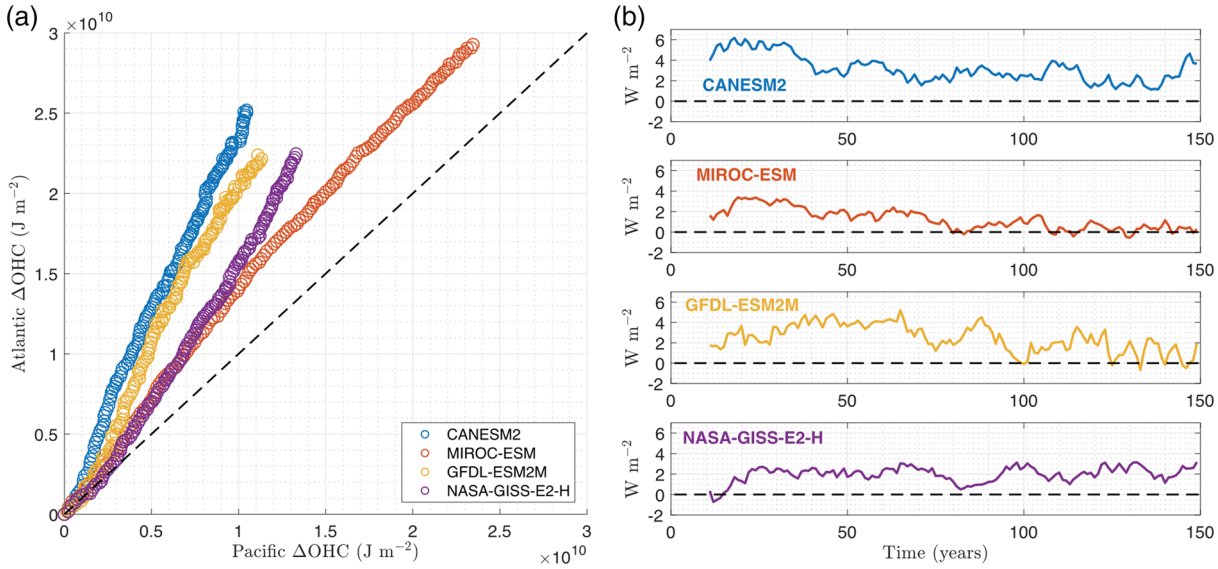

Figure 4. (a) Atlantic versus Pacific top-3-km column-averaged annual OHC anomalies (in J m^{-2}) immediately following an abrupt quadrupling of atmospheric CO_2 in CMIP5 models (each dot represents 1 year). Atlantic and Pacific basins defined from 30°S to 65°N. The deviation from the identity line (black dashed) highlights the Atlantic's enhanced warming rate relative to the Pacific in these experiments. (b) Decadal running means of individual model Atlantic-Pacific heat storage contrasts $\partial_t(\Delta\mathrm{OHC}_{Atl} - \Delta\mathrm{OHC}_{Pac})$ (in W m^{-2}).

causing an increase in the net surface heat flux $\Delta\mathcal{F}_s^{SB}$. However, this additional heat input is then lost to the model southern ocean, which ensures that the heat storage contrast remains stationary.

This heat loss to the model southern ocean is similar to the "redistribution temperature" response seen in Xie and Vallis (2012) where, in an idealized model of the Atlantic ocean, the MOC weakening serves to transport heat from the Northern Hemisphere high latitudes toward the Southern Hemisphere. We note that across CMIP5 models, under historical simulations, the Southern Ocean dominates ocean heat uptake and exports approximately half of the energy it takes up *northwards* (Frölicher et al., 2015); this northward transport is also supported by observations, which results in a delayed warming of the Southern Ocean (Armour et al., 2016). However, a weakening of this northward heat transport (perhaps as a result of ozone hole recovery in the near future) could manifest as an anomalous southward transport from the Atlantic basin to the Southern Ocean, which is consistent with our results.

3.4. Parallels With CMIP5 Models

Our analysis suggests new ways to look at the AMOC's role in ocean heat storage in observations and more complex climate models. We performed a preliminary analysis of four CMIP5 models and show that there is a heat storage contrast between the Atlantic and Pacific basins (defined from 30°S to 65°N) in abrupt CO_2-quadrupling experiments (Figure 4). Under this more intense forcing scenario, the multimodel time-mean heat storage contrast is 2.2 W m^{-2}. Looking at individual models, the contrast persists in the models CANESM2 and NASA-GISS-E2-H but weakens in MIROC-ESM and GFDL-ESM2M (Figure 4b).

This could be due to different model AMOC responses and, particularly, whether the control model AMOC cells are thermally direct (flux heat upward, like the SB MOC) or indirect (flux heat downward). For example, Zika et al. (2013) diagnosed overturning cells in UVic ESM and found that the cell coincident with the AMOC was thermally indirect, so our results might not apply to this model. However, it is still an open question whether the real-world AMOC is thermally direct or indirect (Kuhlbrodt et al., 2007). Nevertheless, we suggest that the AMOC is at least responsible for the existence of a contrast in each of these CMIP5 models, just as the SB MOC is responsible for the contrast in DDrake.

4. Conclusion

In this study, we have used an idealized coupled climate model with two basins (DDrake), with a SB endowed with a MOC akin to that of the present-day Atlantic Ocean, to study the transient response of

the ocean to an abrupt doubling of atmospheric CO_2. We find that the SB experiences an enhanced heat storage rate due to a rapid advection of surface temperature anomalies into its interior. Similar to Kostov et al. (2014), who found no significant correlations between the AMOC weakening and the depth of heat storage in CMIP5 models, we find no significant relationship between the SB's MOC weakening and its weakening heat storage rate in our setup. Moreover, we find that the heat storage contrast between the two basins of DDrake remains almost constant during the period of MOC weakening, and throughout the rest of the simulated 200 years on multidecadal timescales.

Weakening of the AMOC has been seen in proxy observations and climate models (Caesar et al., 2018; Gregory et al., 2005; Rahmstorf et al., 2015; Weaver et al., 2012), and recent observations from RAPID are consistent with a declining AMOC response predicted from coupled climate models (Smeed et al., 2018). It has been suggested that a continued weakening in the future could lead to a loss of this deep ocean heat storage mechanism, resulting in an accelerated warming of surface temperatures (Chen & Tung, 2018). However, this view perhaps focuses too narrowly on $\Delta\Psi_{res}$ and, as we have found in our experiments, considering $\Delta(\Psi_{res}\delta\theta)$ paints a more complicated picture, by introducing differential warming as an additional process to MOC weakening (Equation 1).

Contrary to expectations, we find that the anomalous downward MOC heat flux $\Delta\mathscr{H}_{MOC}$ increases as the SB MOC weakens. Furthermore, we find that the dominant term in its decomposition is from differential warming, with the control overturning playing the prominent role (Figure 3a). Finally, although $\Delta\mathscr{H}_{MOC}$ increases, this does not lead to an increase in the heat storage contrast, as this additional heat input is subsequently lost to the southern ocean region (Figure 3b). Thus, although the presence of a MOC is important for the SB's enhanced heat storage rate, the change in MOC strength is surprisingly unimportant during the simulated 200 years in our experiment. It is not known whether this MOC weakening affects the difference in ΔOHC at equilibrium between the SB and LB; further simulations would be needed to address this.

We emphasise that, like all modeling studies, our results are model dependent. The compensation we found between the $\Delta\Psi_{res}$ terms in Figure 3a very likely depends on model-specific AMOC states and responses. It should also be underlined that this is an idealized model: There is no bottom topography, no Antarctic Bottom Water formation, and the control SB MOC strength is 26.0 Sv, which is ∼40% stronger than the real-world AMOC (Buckley & Marshall, 2016). However, in this simplified setup, we were able to provide a conceptual grasp on how a deep overturning circulation affects a basin's heat storage rate, and the comparison with CMIP5 models in Figure 4 is encouraging. A key conclusion that extends beyond the specifics of our model is that the impact of the AMOC on OHS is driven not only by the AMOC's strength. The temperature structure and its changes must also be considered for a complete evaluation of the AMOC's role.

Our results underline the importance of the AMOC in ocean heat storage, and for its accurate representation in other, predictive climate models. Continued observational monitoring efforts such as RAPID (Smeed et al., 2018) and the Overturning in the Subpolar North Atlantic Program (OSNAP) (Lozier et al., 2019), in conjunction with more advanced high-resolution climate models, should drive a deeper understanding of the AMOC, but we also encourage the use of simpler, more conceptual models such as DDrake in order to make sense of this increasing complexity.

Data Availability Statement

The CMIP5 data used in this paper are available at the Earth System Grid Federation (ESGF) Portal (https://esgf-node.llnl.gov/search/cmip5/).

Acknowledgments

The authors would like to thank Y. Kostov, M. Buckley, R. Emole, and an anonymous reviewer for their useful comments and suggestions. P. Shatwell was supported by the U.K. Engineering and Physical Sciences Research Council (EPSRC) Centre for Doctoral Training in Mathematics of Planet Earth (MPECDT).

References

Adcroft, A., Campin, J.-M., Hill, C., & Marshall, J. (2004). Implementation of an atmosphere–ocean general circulation model on the expanded spherical cube. *Monthly Weather Review*, *132*(12), 2845–2863.

Armour, K. C., Marshall, J., Scott, J. R., Donohoe, A., & Newsom, E. R. (2016). Southern Ocean warming delayed by circumpolar upwelling and equatorward transport. *Nature Geoscience*, *9*(7), 549.

Buckley, M. W., Ferreira, D., Campin, J.-M., Marshall, J., & Tulloch, R. (2012). On the relationship between decadal buoyancy anomalies and variability of the Atlantic meridional overturning circulation. *Journal of Climate*, *25*(23), 8009–8030.

Buckley, M. W., & Marshall, J. (2016). Observations, inferences, and mechanisms of the atlantic meridional overturning circulation: A review. *Reviews of Geophysics*, *54*, 5–63. https://doi.org/10.1002/2015RG000493

Caesar, L., Rahmstorf, S., Robinson, A., Feulner, G., & Saba, V. (2018). Observed fingerprint of a weakening atlantic ocean overturning circulation. *Nature*, *556*(7700), 191.

Chen, X., & Tung, K.-K. (2014). Varying planetary heat sink led to global-warming slowdown and acceleration. *Science*, *345*(6199), 897–903.

Chen, X., & Tung, K.-K. (2018). Global surface warming enhanced by weak Atlantic overturning circulation. *Nature*, *559*(7714), 387.

Desbruyeres, D., McDonagh, E. L., King, B. A., & Thierry, V. (2017). Global and full-depth ocean temperature trends during the early twenty-first century from Argo and repeat hydrography. *Journal of Climate*, *30*(6), 1985–1997.

Drijfhout, S. S., Blaker, A. T., Josey, S. A., Nurser, A. J. G., Sinha, B., & Balmaseda, M. A. (2014). Surface warming hiatus caused by increased heat uptake across multiple ocean basins. *Geophysical Research Letters*, *41*, 7868–7874. https://doi.org/10.1002/2014GL061456

Ferreira, D., & Marshall, J. (2015). Freshwater transport in the coupled ocean-atmosphere system: A passive ocean. *Ocean Dynamics*, *65*(7), 1029–1036.

Ferreira, D., Marshall, J., Bitz, C. M., Solomon, S., & Plumb, A. (2015). Antarctic ocean and sea ice response to ozone depletion: A two-time-scale problem. *Journal of Climate*, *28*(3), 1206–1226.

Ferreira, D., Marshall, J., & Campin, J.-M. (2010). Localization of deep water formation: Role of atmospheric moisture transport and geometrical constraints on ocean circulation. *Journal of Climate*, *23*(6), 1456–1476.

Frölicher, T. L., Sarmiento, J. L., Paynter, D. J., Dunne, J. P., Krasting, J. P., & Winton, M. (2015). Dominance of the Southern Ocean in anthropogenic carbon and heat uptake in CMIP5 models. *Journal of Climate*, *28*(2), 862–886.

Gent, P. R., & Mcwilliams, J. C. (1990). Isopycnal mixing in ocean circulation models. *Journal of Physical Oceanography*, *20*(1), 150–155.

Gregory, J. M., Dixon, K. W., Stouffer, R. J., Weaver, A. J., Driesschaert, E., Eby, M., et al. (2005). A model intercomparison of changes in the Atlantic thermohaline circulation in response to increasing atmospheric CO_2 concentration. *Geophysical Research Letters*, *32*, L12703. https://doi.org/10.1029/2005GL023209

Hansen, J., Sato, M., Kharecha, P., & Schuckmann, K. (2011). Earth's energy imbalance and implications. *Atmospheric Chemistry and Physics*, *11*(24), 13,421–13,449.

Klinger, B. A., Marshall, J., & Send, U. (1996). Representation of convective plumes by vertical adjustment. *Journal of Geophysical Research*, *101*(C8), 18,175–18,182.

Kostov, Y., Armour, K. C., & Marshall, J. (2014). Impact of the Atlantic meridional overturning circulation on ocean heat storage and transient climate change. *Geophysical Research Letters*, *41*, 2108–2116. https://doi.org/10.1002/2013GL058998

Kuhlbrodt, T., Griesel, A., Montoya, M., Levermann, A., Hofmann, M., & Rahmstorf, S. (2007). On the driving processes of the Atlantic meridional overturning circulation. *Reviews of Geophysics*, *45*, RG2001. https://doi.org/10.1029/2004RG000166

Liu, W., Xie, S.-P., Liu, Z., & Zhu, J. (2017). Overlooked possibility of a collapsed Atlantic meridional overturning circulation in warming climate. *Science Advances*, *3*(1), e1601666.

Lozier, M. S., Li, F., Bacon, S., Bahr, F., Bower, A. S., Cunningham, S. A., et al. (2019). A sea change in our view of overturning in the subpolar North Atlantic. *Science*, *363*(6426), 516–521.

Marshall, J., Adcroft, A., Hill, C., Perelman, L., & Heisey, C. (1997). A finite-volume, incompressible Navier Stokes model for studies of the ocean on parallel computers. *Journal of Geophysical Research*, *102*(C3), 5753–5766.

Marshall, J., Hill, C., Perelman, L., & Adcroft, A. (1997). Hydrostatic, quasi-hydrostatic, and nonhydrostatic ocean modeling. *Journal of Geophysical Research*, *102*(C3), 5733–5752.

Marshall, J., Scott, J. R., Armour, K. C., Campin, J.-M., Kelley, M., & Romanou, A. (2015). The oceans role in the transient response of climate to abrupt greenhouse gas forcing. *Climate Dynamics*, *44*(7-8), 2287–2299.

Meehl, G. A., Arblaster, J. M., Fasullo, J. T., Hu, A., & Trenberth, K. E. (2011). Model-based evidence of deep-ocean heat uptake during surface-temperature hiatus periods. *Nature Climate Change*, *1*(7), 360.

Molteni, F. (2003). Atmospheric simulations using a GCM with simplified physical parametrizations. I: Model climatology and variability in multi-decadal experiments. *Climate Dynamics*, *20*(2-3), 175–191.

Myhre, G., Highwood, E. J., Shine, K. P., & Stordal, F. (1998). New estimates of radiative forcing due to well mixed greenhouse gases. *Geophysical Research Letters*, *25*(14), 2715–2718.

Rahmstorf, S., Box, J. E., Feulner, G., Mann, M. E., Robinson, A., Rutherford, S., & Schaffernicht, E. J. (2015). Exceptional twentieth-century slowdown in atlantic ocean overturning circulation. *Nature Climate Change*, *5*(5), 475.

Redi, M. H. (1982). Oceanic isopycnal mixing by coordinate rotation. *Journal of Physical Oceanography*, *12*(10), 1154–1158.

Rhein, M., Rintoul, S. R., Aoki, S., Campos, E., Chambers, D., Feely, R. A., et al. (2013). Observations: Ocean. In T. F. Stocker et al. (Eds.), *Climate Change 2013: the Physical Science Basis. Contribution of Working Group I to the Fifth Assessment Report of the Intergovernmental Panel on Climate Change*. Cambridge, United Kingdom and New York, NY, USA: Cambridge University Press.

Saenko, O. A., Yang, D., & Gregory, J. M. (2018). Impact of mesoscale eddy transfer on heat uptake in an eddy-parameterizing ocean model. *Journal of Climate*, *31*(20), 8589–8606.

Smeed, D. A., Josey, S. A., Beaulieu, C., Johns, W. E., Moat, B. I., Frajka-Williams, E., et al. (2018). The North Atlantic ocean is in a state of reduced overturning. *Geophysical Research Letters*, *45*, 1527–1533. https://doi.org/10.1002/2017GL076350

Trenberth, K. E., Fasullo, J. T., & Balmaseda, M. A. (2014). Earths energy imbalance. *Journal of Climate*, *27*(9), 3129–3144.

Von Schuckmann, K., Palmer, M. D., Trenberth, K. E., Cazenave, A., Chambers, D., Champollion, N., et al. (2016). An imperative to monitor Earth's energy imbalance. *Nature Climate Change*, *6*(2), 138.

Watanabe, M., Kamae, Y., Yoshimori, M., Oka, A., Sato, M., Ishii, M., et al. (2013). Strengthening of ocean heat uptake efficiency associated with the recent climate hiatus. *Geophysical Research Letters*, *40*, 3175–3179. https://doi.org/10.1002/grl.50541

Weaver, A. J., Sedláček, J., Eby, M., Alexander, K., Crespin, E., Fichefet, T., et al. (2012). Stability of the Atlantic meridional overturning circulation: A model intercomparison. *Geophysical Research Letters*, *39*, L20709. https://doi.org/10.1029/2012GL053763

Winton, M. (2000). A reformulated three-layer sea ice model. *Journal of Atmospheric and Oceanic Technology*, *17*(4), 525–531.

Winton, M., Griffies, S. M., Samuels, B. L., Sarmiento, J. L., & Frölicher, T. L. (2013). Connecting changing ocean circulation with changing climate. *Journal of climate*, *26*(7), 2268–2278.

Xie, P., & Vallis, G. K. (2012). The passive and active nature of ocean heat uptake in idealized climate change experiments. *Climate Dynamics*, *38*(3-4), 667–684.

Zanna, L., Khatiwala, S., Gregory, J. M., Ison, J., & Heimbach, P. (2019). Global reconstruction of historical ocean heat storage and transport. *Proceedings of the National Academy of Sciences*, *116*(4), 1126–1131.

Zika, J. D., Sijp, W. P., & England, M. H. (2013). Vertical heat transport by ocean circulation and the role of mechanical and haline forcing. *Journal of Physical Oceanography*, *43*(10), 2095–2112.